AIAA 82-4157

Holographic Interferometry Near Gas/Liquid Critical Points

H. Klein* and K. Wanders†
Deutsche Forschungs und Versuchanstalt für Luft und Raumfahrt, Cologne, Federal Republic of Germany

Facilities for the examination of critical phenomena are substantially extended by access to the reduced-gravity environment in space. First, however, it seems desirable to demonstrate the advantages of experimentation in space by, for example, measuring the extremely sensitive density profiles of critical fluid samples under the influence of reduced gravity onboard Spacelab. The objective of this work is to illustrate that such measurements may be conveniently performed by holographic interferometry. The fluid under investigation ($CClF_3$ with a critical overall density) is cooled from temperatures above the critical temperature. Changes in the density profile induced by gravity and temperature gradients are visualized by holographic interferometry. The interferometric patterns are analyzed in terms of the theory of critical phenomena. Two different means by which temperature gradients may arise in critical samples have been revealed in our experiments: convection and adiabatic changes in the density distribution.

Nomenclature

D = geometric path length of light in the sample
g = gravitational acceleration
h = coordinate parallel to g in the sample
h_c = position in the sample where the local density is equal to the critical density
n = refractive index
n_c = refractive index at the critical point
n_c' = $(\partial n/\partial \rho)$ at the critical point
p = pressure
p_c = critical pressure
T = temperature
T_c = critical temperature
ΔT^* = $(T-T_c)/T_c$
γ = critical exponent of the isothermal compressibility
Γ = critical amplitude of the isothermal compressibility
λ_0 = wavelength of light in vacuum
ρ = density
ρ_c = critical density
$\Delta\rho^*$ = $(\rho-\rho_c)/\rho_c$
ϕ = phase shift of light

Introduction

WHEN approaching gas/liquid critical points, gravity-induced density distributions in one-component fluids become more and more inhomogeneous.[1] This phenomenon results from the response of density to a fluid specimen's own weight. The fluid's compressibility (response function) diverges at the critical point. Figure 1 shows typical density distributions in a sample (e.g., $CClF_3$) of critical overall density near the critical temperature. The curves are evaluated using the NBS equation of state.[2] In the center of the sample the local density is equal to the critical density. At this position, a density gradient is established which becomes increasingly steeper as the critical temperature is approached, while local densities outside the center are becoming more and more different from the critical density. As a result, diverging differences arise between the experimental values of the physical quantities (e.g., compressibility, specific heat, etc.) obtained under the influence of gravity and the theoretical values assumed for homogeneous samples. This shows why experiments performed under reduced gravity in Spacelab are so advantageous: reduction of gravity reduces the sample's own weight so that any disturbing inhomogeneities with in the samples will arise only at correspondingly larger compressibilities, i.e., closer to the critical point.

The density distributions depicted in Fig. 1 apply only for thermodynamic equilibrium. Establishment of a thermodynamic equilibrium, however, is often slowed or even restrained by temperature gradients which may evolve due to density changes caused by temperature variations. The effect of temperature gradients in this connection is similar to that of gravity. This fact will be demonstrated in our experiments using holographic methods.

In the ground experiments described in this paper, a $CClF_3$ sample of critical overall density is cooled starting from temperatures some degrees above the critical temperature. The resulting changes in the density distribution are associated with corresponding changes of the refractive index

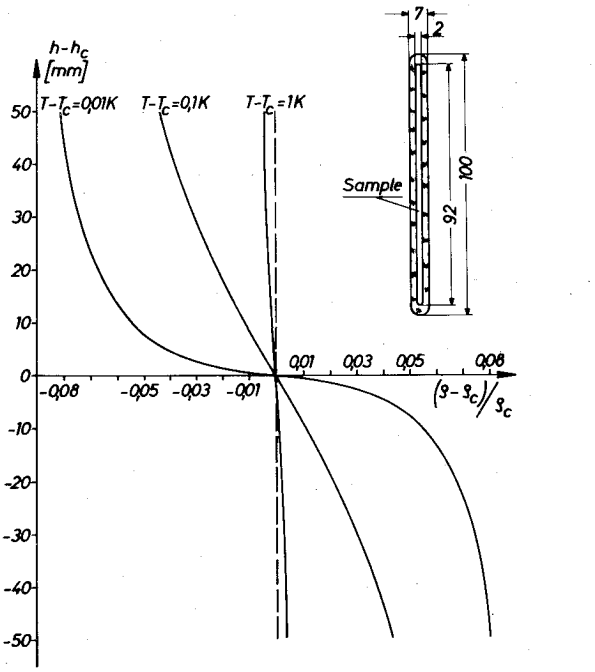

Fig. 1 Gravity-induced density distributions as a function of height in $CClF_3$ at different temperatures T near the critical temperature T_c. The curves are evaluated using the NBS equation of state.[2] The insert shows a draft of the glass capillary in which the $CClF_3$ sample under investigation is enclosed.

Received Aug. 19, 1981; revision received Dec. 8, 1981.

*Scientific Staff, Institute for Space Simulation.
†Scientific Staff, Advanced Programmes Division.

distribution. Refractive index variations lead to proportional phase shifts of the light traversing the sample. Phase shifts of light are measured by means of holographic interferometry. The interference pattern is used to identify changes of the density distribution.

An extensive literature is available dealing with gravity-induced influences on fluids at critical points (see in particular the bibliography in the article by Moldover et al.[1]). Although holographic interferometry is a well-known method for measuring temperature, concentration, and density differences in transparent media,[3,4] little use has been made of this technique in connection with critical phenomena. Indeed, we are aware of only one article[5] which gives a short description of holography as an alternative method to examine density distributions near critical points.

The advantages of holography over the classical interferometric methods are: 1) immediate indication of changes in the sample's structure; 2) easy handling; and 3) except for transparency, no requirements regarding the optical quality of the viewing windows.

Theory

Along the critical isochore, near the critical temperature, the isothermal compressibility of a one-component fluid has the following functional form[1]

$$\rho^{-1}(\partial\rho/\partial p)_T = \Gamma \mid \Delta T^* \mid^{-\gamma} \tag{1}$$

According to the universality hypothesis of critical phenomena, the same value of γ is valid for all gases $(1.2<\gamma<1.3)$.[1]

Under the influence of gravity, the local value of density varies with the vertical coordinate h in the following way:

$$(\partial p/\partial\rho)_T \mathrm{d}\rho = -\rho g \mathrm{d}h \tag{2}$$

Equations (1) and (2) give

$$\partial\rho/\partial h = -\rho^2 g\Gamma \mid \Delta T^* \mid^{-\gamma} \tag{3}$$

Equation (3) states that gravity-induced density gradients are strongly divergent at the gas/liquid critical point.

A relation analogous to Eq. (3) may be derived for temperature gradients replacing the gravitational acceleration constant g. Parallel to a temperature gradient $(\partial T/\partial h)$ the local density in the medium varies in the following way:

$$(\partial T/\partial\rho)_p \mathrm{d}\rho = (\partial T/\partial h)\mathrm{d}h \tag{4}$$

Using the thermodynamic equation

$$\rho^{-1}(\partial\rho/\partial T)_p = -(\partial p/\partial T)_\rho \rho^{-1}(\partial\rho/\partial p)_T \tag{5}$$

and the following relation derived from v.d. Waals' equation

$$(\partial p/\partial T)_{\rho_c} = 4p_c/T_c \tag{6}$$

which is valid for most gases and particularly for $CClF_3$, we find from Eqs. (4) and (1)

$$\partial\rho/\partial h = -\rho(\partial T/\partial h)4(p_c/T_c)\Gamma \mid \Delta T^* \mid^{-\gamma} \tag{7}$$

Equation (7) states that density gradients induced by temperature gradients are strongly divergent at the gas/liquid critical point.

Equations (3) and (7) are valid only at those positions where the local density is equal to the critical density (see Fig. 1). Equations (3) and (7) show that the disturbing influence of gravity on the density distribution near critical points may be canceled by matched temperature gradients. In the presence of temperature gradients, however, samples would not be in thermodynamic equilibrium.

Density variations [e.g., implied in the temperature dependence of Eqs. (3) and (7)] are visualized in our experiments by holographic interferometry via refractive index variations and phase shifts of light.

Refractive index and density are connected by the Lorentz-Lorenz relation

$$(n^2-1)/(n^2+2) = a\rho \tag{8}$$

The factor a is assumed to be constant and unaffected by the critical behavior of the fluid. For densities close to the critical density, we approximate[1]

$$n = n_c + n_c'\Delta\rho^* \tag{9}$$

Taking into account that the refractive index equals the ratio of the wavelength of light in a vacuum to that in the sample with the refractive index n, we get from Eq. (9) the phase shift of light after having traversed the sample: first with the density ρ and second with the density ρ_c

$$\phi = (Dn_c'/\lambda_0)\Delta\rho^* \tag{10}$$

Using Eq. (10) and approximating the differential quotients in Eqs. (3) and (7) by difference quotients, we find for the phase shift of light relative to the position h_c in the sample

1) Under the influence of gravity

$$\phi = -Dn_c' g\Gamma\rho\lambda_0^{-1} \mid \Delta T^* \mid^{-\gamma}\Delta h \tag{11}$$

2) Under the influence of a temperature gradient

$$\phi = -Dn_c'(\partial T/\partial h)4(p_c/T_c)\Gamma\lambda_0^{-1} \mid \Delta T^* \mid^{-\gamma}\Delta h \tag{12}$$

where $\Delta h = h - h_c$. h_c is that position in the sample where the local density is equal to the critical density.

We define the phase shift of light at the position h after a specified temperature variation (from ΔT_1^* to ΔT_2^*)

$$[\Delta\phi]_h \equiv \phi(h,\Delta T_1^*) - \phi(h,\Delta T_2^*) \tag{13}$$

The position difference $[h_{\mathrm{I}} - h_{\mathrm{II}}]_I$, for which the phase shift $([\Delta\phi]_{h_{\mathrm{I}}} - [\Delta\phi]_{h_{\mathrm{II}}})$ amounts to one wavelength of light, is as follows:

1) for Eq. (11)

$$[h_{\mathrm{I}} - h_{\mathrm{II}}]_I = \lambda_0 (Dn_c' g\Gamma\rho)^{-1} \frac{\mid \Delta T_1^* \mid^\gamma \mid \Delta T_2^* \mid^\gamma}{\mid \Delta T_1^* \mid^\gamma - \mid \Delta T_2^* \mid^\gamma} \tag{14}$$

2) for Eq. (12)

$$[h_{\mathrm{I}} - h_{\mathrm{II}}]_I = \lambda_0 \left(Dn_c' \frac{\partial T}{\partial h} 4 \frac{p_c}{T_c}\Gamma\right)^{-1} \frac{\mid \Delta T_1^* \mid^\gamma \mid \Delta T_2^* \mid^\gamma}{\mid \Delta T_1^* \mid^\gamma - \mid \Delta T_2^* \mid^\gamma} \tag{15}$$

Light rays are bent by refractive index gradients in fluids. This effect has not been taken into account in Eqs. (11-15), since for our experimental arrangement it would be of importance only in the temperature range $(T - T_c) < 10^{-2}$ °C which was not analyzed in our study.

Inserting the values applicable to our experiment:

λ_0	$= 632.8$ nm	p_c	$= 39.41$ kp/cm^2 (Ref. 8)
g	$= 10$ m/s^2	n_c	$= 1.0996$ (Ref. 6)
ρ_c	$= 0.581$ g/cm^3 (Ref. 8)	γ	$= 1.275$ (Ref. 7)
D	$= 2$ mm	T_c	$= 302$ K (Ref. 6)
Γ	$= 7.4\times10^{-4}$ cm^2/kp (Ref. 7)		

we get

1) for Eq. (14)

$$[h_{\mathrm{I}}-h_{\mathrm{II}}]_I = 7.2\times 10^4 \frac{|\Delta T_1^*|^{1.275}\,|\Delta T_2^*|^{1.275}}{|\Delta T_1^*|^{1.275}-|\Delta T_2^*|^{1.275}} \text{ mm} \qquad (16)$$

2) for Eq. (15)

$$[h_{\mathrm{I}}-h_{\mathrm{II}}]_I = 8.1\times(\partial h/\partial T)\frac{|\Delta T_1^*|^{1.275}\,|\Delta T_2^*|^{1.275}}{|\Delta T_1^*|^{1.275}-|\Delta T_2^*|^{1.275}} \text{ mm} \qquad (17)$$

Experiment Implementation

The analyzed $CClF_3$ sample is sealed into a DURAN glass capillary tube (external diameter 6.6 mm, internal diameter 2.0 mm, internal height 92.0 mm).[9] The temperature T_c and the position h_c, where the meniscus occurs for the first time, were determined very carefully, as follows.

$T_c = 28.728°C$ and $h_c = 45.9$ mm; T_c is in good agreement with the values given in the literature for the critical temperature ($T_c = 28.715°C$),[6] a fact pointing to the sample's purity. From h_c deviating only by 0.1 mm from the center of the sample, it follows that the overall density of the sample differs by approximately 0.01% from the critical density.[10]

The sample is thermostated in an electronically controlled double thermostat equipped with two opposite windows so that the sample can be observed by the transmitted light. The temperature stability over several hours is better than 10^{-3} K. The temperature gradients along the sample caused by the thermostat are less than 10^{-4} K/cm.

The holographic interferometer is shown in Fig. 2. The laser beam (vacuum wavelength $\lambda_0 = 632.8$ nm) is split into an object beam and a reference beam. After passing through the scattering screen (diffusor) and the thermostated sample, the expanded object beam impinges upon the photoplate where it interferes with the expanded reference beam. This brings about the storage of a light wave's amplitude and phase, a characteristic feature of holography. The desired holographic interferogram is obtained through double exposure of the photoplate and subsequent reconstruction by the reference beam. The first exposure of the photoplate is made at the temperature $T_c+\Delta T_1$ (zero hologram). Thus the density profile at $T_c+\Delta T_1$ is stored by means of the phase of the object wave. The second exposure of the photoplate is at $T_c+\Delta T_2$, which provides for storage of the density profile of the sample at $T_c+\Delta T_2$ as well. The structure generated by the double exposure on the photoplate is fixed. By diffraction of the reference beam on this structure, both density profiles are reconstructed in such a way that the original object waves with their different phases are superimposed. This leads to a strip pattern. A dark strip indicates that at this point the phases of the object waves, at the temperatures $T_c+\Delta T_1$ and $T_c+\Delta T_2$, differ by an odd multiple of the light's half wavelength. Several test runs were carried out with partly different cooling rates. The samples were first heated to approximately 31°C and maintained at this temperature for several hours. Then the samples were started to be cooled. During the cooling process several hologram plates were exposed whose zero holograms were each recorded at the same temperature $T_c+\Delta T_1$. After the first exposure, the hologram plates were sealed to be lightproof. The second exposure was made at a temperature $T_c+\Delta T_2$ ($T_c < T_c+\Delta T_2 < T_c+\Delta T_1$), which was different for each hologram plate.

Changes of the optical properties of the DURAN glass capillary in the course of an experimental run were sufficiently small as to not affect the holograms.

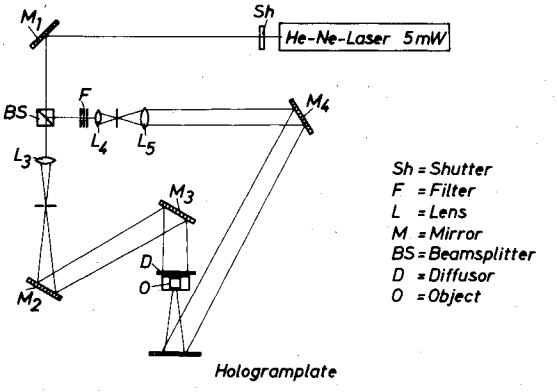

Fig. 2 Schematic diagram of the holographic interferometer.

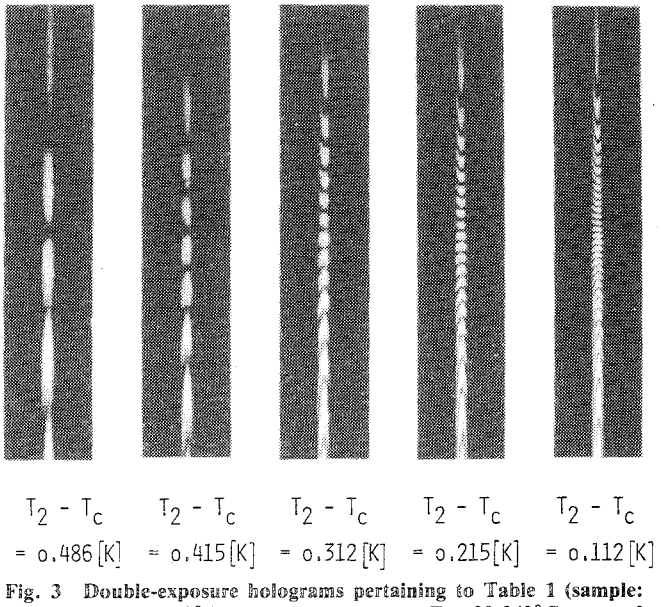

Fig. 3 Double-exposure holograms pertaining to Table 1 (sample: $CClF_3$, $T_c = 28.728°C$, zero hologram at $T_1 = 29.342°C$, second exposure at T_2, cooling rate $= 7\times 10^{-3}$ K/min).

Test Results

The interferograms obtained all have the same qualitative appearance (see Fig. 3): concentration of the interference strips at the point h_c where the local density of the sample equals the critical density. Above this point the interference strips are bent downward, below this point they are bent upward. The concentration of the interference strips at the point h_c increases when the critical temperature ($\Delta T_2 \to 0$) is being approached. For two cooling rates Tables 1 and 2 show the strip distances at the point h_c at different temperatures.

Discussion

For a qualitative interpretation of the interference patterns obtained we assume the coordinate $\Delta\rho^*$ in Fig. 1 to be replaced by ϕ [according to Eq. (10), $\Delta\rho^*$ and ϕ differ by a constant factor]. In the holograms, two $\phi(h)$ curves are compared with each other in each case. If, for a given h, the distance between the two curves is an odd multiple of half the wavelength of light, a dark interference strip appears at this point. The vicinity of h_c is characterized by a maximum decrease of this distance so that a concentration of the interference strips occurs here which increases when T_c is being approached. In our experiment, the form of the interference lines is due to the cylindrical shape of the capillary tube containing our test substance. In the center of the capillary

Table 1 Interference strip distances at point h_c where local density is equal to critical density (sample: $CClF_3$)[a]

$\Delta T_2 = T_2 - T_c$, K	Strip distance, mm, according to Experiment	Eq. (16)	Eq. (17) with $\partial T/\partial h = 0.011$ K/cm
0.486	8.0	76.7	7.9
0.415	3.2	41.1	4.2
0.312	1.6	19.4	2.0
0.215	1.0	9.5	1.0
0.112	0.6	3.4	0.4

[a] $T_c = 28.728$°C, cooling rate $= 7 \times 10^{-3}$ K/min, zero hologram at $T_1 = 29.342$°C, second exposure at T_2.

Table 2 Interference strip distances at point h_c where local density is equal to critical density (sample: $CClF_3$)[a]

$\Delta T_2 = T_2 - T_c$, K	Strip distance, mm, according to Experiment	Eq. (16)
0.498	90	95
0.395	26.5	36.5
0.292	15.5	17.1
0.196	10.5	8.2
0.092	7.2	2.6
0.010	5.0	0.14

[a] $T_c = 28.728$°C, cooling rate $= 3 \times 10^{-3}$ K/min, zero hologram at $T_1 = 29.33$°C, second exposure at T_2.

tube, the path D traveled by the light at a given height h through the sample, is equal to the tube's internal diameter and toward the sides it decreases toward zero. According to Eq. (10), this means that the phases decrease as well. Since an interference strip is in a position of constant phase difference, it curves into the direction of increasing density difference when the geometric path D is reduced. According to Fig. 1, this corresponds above h_c to a downward bending and below h_c to an upward bending.

Table 1 presents a relatively fast cooling process of the analyzed critical $CClF_3$ sample. The cooling rate is 7×10^{-3} K/min. In the center of the sample (h_c), where the local density is equal to the critical density, the distance between the interference strips is only about 1/10th of the value anticipated according to Eq. (16) for our sample in thermal equilibrium under the effect of gravity. The reason for this discrepancy is a temperature gradient generated by "conventional convection"[11] in the sample: due to the rapid cooling, a relatively large temperature gradient perpendicular to the gravitational field is induced in the layers of the sample matter directly adjacent to the capillary tube's inner wall. The immediate effect is "conventional convection" during which cold matter is accumulating in the lower part of the sample and warm matter is mounting to the top. Thus a temperature gradient is generated in the center of the sample. This temperature gradient can be calculated by substituting the measured strip distance in Eq. (17). The experimental strip distances of Table 1 are consistent with the temperature gradient $\partial T/\partial h = 0.011$ K/cm antiparallel to g.

Table 2 is a typical example of a relatively slow cooling process. The cooling rate is 3×10^{-3} K/min, i.e., less than half the rate in Table 1. Under these conditions, the temperature gradient perpendicular to gravity induced by the cooling process is very small and convection is correspondingly small, so that only a very-low-temperature gradient can occur. Therefore, the first four strip distances of Table 2 are in good agreement with the values calculated by means of Eq. (16). The last two experimental strip distances in Table 2 are markedly larger than the theoretical values obtained with Eq. (16). These two values are in the range $(T_2 - T_c) < 0.1$ K. In this range we have an intensified occurrence of the adiabatic temperature gradient parallel to the gravitational field, which is characteristic of critical samples under the influence of gravity[1]: $(\partial T/\partial h)_s = -\rho g (\partial T/\partial p)_s$. Near the critical point $(\partial T/\partial p)_s$ may be substituted by $(\partial T/\partial p)_{\rho_c}$.

From Eq. (6) and the above-mentioned critical values for $CClF_3$ it follows that the adiabatic temperature gradient may be as much as 10^{-3} K/cm. If we substitute this value into Eq. (17) and take into account that $(\partial T/\partial h)_s$ is parallel to g, we find that in this way a considerable reduction and/or elimination is possible of the influence of gravity on the density profile. This effect applies for the last two values in Table 2. Establishment of the thermodynamically stable equilibrium [i.e., values for strip distances according to Eq. (16)] takes more than 20 h. This is, however, the limit to which we are capable of keeping our equipment in thermal stability and free from vibrations.

Acknowledgment

We are greatly indebted to Prof. F. Becker for preparing the $CClF_3$ probe. H. J. Juraschek and W. K. Feibig have supported us with technical assistance. Dr. G. P. Görler has given some valuable suggestions for designing the thermostat.

References

[1] Moldover, M. R., Sengers, J. V., Gammon, R. W., and Hocken, R. J., "Gravity Effects in Fluids near Gas-Liquid Critical Point," *Review of Modern Physics,* Vol. 51, Jan. 1979, pp. 79-99.

[2] Sengers, J. V. and Levelt Sengers, J. M. H., "Critical Phenomena in Classical Fluids," *Progress in Liquid Physics,* edited by C. A. Croxton, John Wiley & Sons, New York, 1978, pp. 103-174.

[3] Vest, Ch. M., *Holographic Interferometry,* John Wiley & Sons, New York, Chichester, Brisbane, Toronto, 1979.

[4] Oshima, K. and Hara, T., "Fluid Dynamic Measurements Using Holographic Interferometry," *Proceedings of the 2nd Symposium on Flow Visualization,* ISAS, University of Tokyo, Japan, July 1974, pp. 47-55.

[5] Estler, W. T., Hocken, R., Charlton, T., and Wilcox, L. R., "Coexistence Curve, Compressibility, and the Equation of State of Xenon near the Critical Point," *Physical Review,* Ser. A, Vol. 12, Nov. 1975, pp. 2118-2136.

[6] Levelt Sengers, J. M. H., Straub, J., and Vicentini-Missoni, M., "Coexistence Curves of CO_2, N_2O, and C Cl F_3 in the Critical Region," *Journal of Chemical Physics,* Vol. 54, June 1971, pp. 5034-5050.

[7] Schoenes, F. J., "Light Scattering and Absolute Determination of the Compressibility of C Cl F_3 near the Critical Points," *Berichte der Bunsengesellschaft,* Vol. 76, 1976, pp. 228-231.

[8] Becker, F., Private communication, University of Frankfurt, June 1980.

[9] Becker, F., Sample preparation, University of Frankfurt, June 1980.

[10] Moldover, M. R., "Visual Observation of the Critical Temperature and Density: CO_2 and C_2H_4," *Journal of Chemical Physics,* Vol. 61, Sept. 1974, pp. 1766-1778.

[11] Ostrach, S., "Convection Phenomena at Reduced Gravity of Importance for Materials Processing," ESA Special Publication 114, 1974, pp. 41-56.